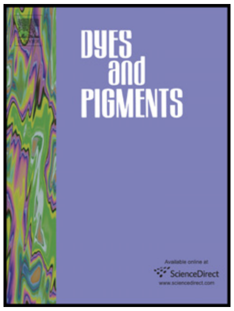

Single-Wall Carbon Nanotubes Covalently Linked with Zinc (II) Phthalocyanine Bearing Poly (aryl benzyl ether) Dendritic Substituents: Synthesis, Characterization and Photoinduced Electron Transfer

Dandan He, Yiru Peng, Hongqin Yang, Dongdong Ma, Yuhua Wang, Kuizhi Chen, Pingping Chen, Jiafang Shi

PII: S0143-7208(13)00168-X

DOI: 10.1016/j.dyepig.2013.05.003

Reference: DYPI 3940

To appear in: *Dyes and Pigments*

Received Date: 21 January 2013

Revised Date: 2 May 2013

Accepted Date: 2 May 2013

Please cite this article as: He D, Peng Y, Yang H, Ma D, Wang Y, Chen K, Chen P, Shi J, Single-Wall Carbon Nanotubes Covalently Linked with Zinc (II) Phthalocyanine Bearing Poly (aryl benzyl ether) Dendritic Substituents: Synthesis, Characterization and Photoinduced Electron Transfer, *Dyes and Pigments* (2013), doi: 10.1016/j.dyepig.2013.05.003.

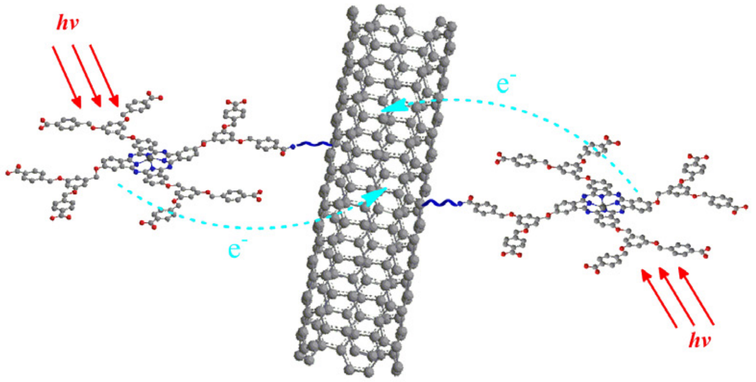
hν
e⁻
e⁻
hν

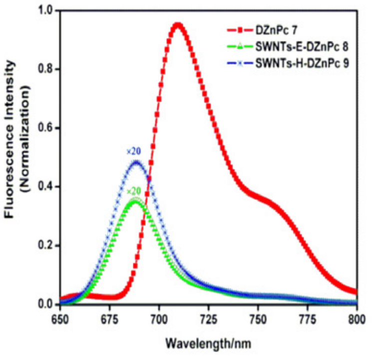
Fluorescence Intensity (Normalization)
Wavelength/nm
DZnPc 7
SWNTs-E-DZnPc 8
SWNTs-H-DZnPc 9
×20
×20
0.0
0.2
0.4
0.6
0.8
1.0
650
675
700
725
750
775
800

Highlights:

- Synthesis a series of dendritic phthalocyanine-spacer linker-SWNTs nanoconjugates.
- Intramolecular electron transfer could occur from phthalocyanines to SWNTs.
- Electron transfer rate and efficacy increase with decreasing spacer linker length.

Single-Wall Carbon Nanotubes Covalently Linked with Zinc (II) Phthalocyanine Bearing Poly (aryl benzyl ether) Dendritic Substituents: Synthesis, Characterization and Photoinduced Electron Transfer

Dandan He[1], Yiru Peng[*1], Hongqin Yang[2], Dongdong Ma[1], Yuhua Wang[2], Kuizhi Chen[1],

Pingping Chen[1], Jiafang Shi[1]

[1]College of Chemistry and Chemical Engineering, Fujian Provincial Key Laboratory of Polymer Materials, Fujian Normal University, Fuzhou 350007, China

[2]Key Lab of Optoelectronic Science and Technology for Medicine of Ministry of Education, Fujian Normal University, Fuzhou 350007, China

Abstract：A novel series of dendritic phthalocyanine-single-wall carbon nanotube nanoconjugates, zinc (II) phthalocyanine bearing poly (aryl benzyl ether) dendritic substituents covalently linked with single-wall carbon nanotubes through either ethylenediamine or hexamethylenediamine as the spacer linker, were prepared. The structures and morphologies of the dendritic phthalocyanine-single-wall carbon nanotube nanoconjugates were characterized by IR, Raman spectroscopy, transmission electron microscopy and thermal gravimetric analysis methods. The photophysical properties of the nanoconjugates were studied by steady-state and time-resolved fluorescence spectroscopy. The intramolecular electron transfer occurred from phthalocyanine (donor) to the carbon nanotubes (acceptor) by a photoinduced process. The electron transfer exchange rate constant and the electron

---

[*] Corresponding author. Tel.: + 86 591 8346 5156.
E-mail address: yirupeng@fjnu.edu.cn (Y. Peng).

transfer efficacy between the dendritic phthalocyanine and single-wall carbon nanotubes increased with decreasing length of spacer linker. These novel nanoconjugates were fundamentally important due to the synergy effects of carbon nanotubes and dendritic zinc phthalocyanine, which may find potential application as biological labels.

Keywords: Single-wall carbon nanotubes; Dendrimer; Phthalocyanine; Photoinduced electron transfer; Photophysical properties; Synthesis

1. Introduction

Single-wall carbon nanotubes (SWNTs) have unique electronic, mechanism and structural properties as well as chemical stability that make them ideal nano-materials for applications in energy conversion, gas storage, sensing and biological applications [1-2]. However, processing SWNTs and integrating them in real world applications were severely limited by a number of inherent shortcomings: purification, manipulation and low solubility in organic solvents. In order to improve their solubility and overcome the aggregation properties, various functionalized strategies, like covalent [3-5] and noncovalent methods [6-9] were employed. For example, Gudi et al., reported on the functionalization of SWNTs with ferrocene species, and on the result of a spectroscopic investigation suggested an intramolecular electron transfer in the functionalized nanotubes [10]. Sun and coworkers functionalized SWNTs with pyrene-containing dendra and found that the photo-excited pyrene moieties were quenched by linked SWNTs via efficient intramolecular energy transfer [11]. Some previous work has been reported on the preparation of phthalocyanine-SWNTs composites or nanoconjugates and their photoinduced intramolecular electron transfer properties [12-17].

A dendritic phthalocyanine is a metal complex encapsulated within the inner core of a dendrimer bearing hydrophilic surface groups, which is considered as a new efficient light-harvesting system. Functionalization of the SWNTs with a light-harvesting dendritic phthalocyanine would present a particular strategy to attach a limited number of function groups onto the SWNTs surface, thus we expected them to show better solubility, less aggregation and better photophysical properties. Besides, functionalized SWNTs with electron-donor antenna chromophores through a covalent linkage which may lead to a significant breakthrough in generating singlet excited energy and conversion into chemical energy, leading to excellent electron-transfer properties. However, at present, there are few examples of dendritic phthalocyanine functionalized carbon nanotubes reported.

In this paper, a novel series of dendritic phthalocyanine-SWNTs nanoconjugates, zinc (II) phthalocyanine bearing poly (aryl benzyl ether) dendritic substituents covalently linked with SWNTs through either ethylenediamine or hexamethylenediamine as the spacer linker, were synthesized and characterized. The photophysical and photoinduced electron transfer properties of this novel series of dendritic phthalocyanine-SWNTs nanoconjugates were studied by UV/Vis, steady-state and time-resolved fluorescence spectroscopy.

2 Materials and Methods

Solvents for organic synthesis were reagent grade, and were dried according standard procedures. All the other compounds were used as received. SWNTs-COOH: diameter of about 20 nm, a length of 1-3 μm and purity > 90%.

Raman spectra were measured at room temperature with a Renishaw micro-Raman spectroscopic system (Renishaw Invia, UK) and a diode laser operating at a wavelength of 785 nm as an excitation source. The UV/Vis spectra were recorded with a Cary50 UV/Vis spectrophotometer. A Perkin-Elmer ATR Fourier transform infrared spectrophotometer was used for IR data collection. Steady-state and time-resolved fluorescence spectra were carried out on a FL900/FS920 fluorescence spectrophotometer. Thermal properties of the samples were measured using a Mettler-Toledo TGA/SDTA851e at a heating rate of 10□/min in nitrogen atmosphere. Transmission electron microscopy images were recorded on a JEM-2010 transmission electron microscope at 200 kV accelerating voltage.

3 Experimental

3.1 Synthesis of compound 1

Compound 1 and **Compound 2** were synthesized according to the literature [18,19]. *N*-*tert*-butyloxycarbonyl-1,2-ethylenediamine (*N*-Boc-ethylenediamine) was obtained by treatment of 1,2-ethylenediamine (12 mL, 200 mmol) with *di*-*tert*-butyldicarbonate (23.2 mL, 100 mmol) in anhydrous methanol (120 mL) at room temperature. The mixture was evaporated to dryness under reduced pressure. The residue was dissolved in water (100 mL) and saturated with sodium carbonate. The aqueous layer was exacted with ethyl acetate (40 mL) by three times. The combined organic layers were dried by magnesium sulfate anhydrous and evaporated to give **compound 1** as yellow oil. Yield (16.00 g), percentage yield (50 %). IR/cm^{-1}: 3446, 2976, 2930, 1692, 1365, 1397, 1170, 1039, 955, 870. ^{1}H NMR (CDCl$_3$, 400MHz, δ/ppm): 5.00 (s, 1H, -NH-), 3.18 (t, 2H, -NHCH$_2$-), 2.80 (t, 2H, -CH$_2$- close to amino), 1.45 (s, 9H, -CH$_3$), 1.40 (s, 2H, -NH$_2$). ESI-MS (m/z): 160. Found: 161 $[M+H]^+$.Analysis calcd. For $C_7H_{16}N_2O_2$, C: 52.50, H: 10.00, N: 17.50. Found: C: 52.54, H: 10.05, N: 17.53. [See SI-Fig.1-3]

3.2 Synthesis of compound 2

N-tert-butyloxycarbonyl-1,2-hexamethylenediamine (*N*-Boc-hexamethylenediamine) was obtained by treatment of 1,2-hexamethylenediamine (9.30 g, 80 mmol) with *di-tert*-butyl dicarbonate (9.28 mL, 40 mmol) in anhydrous methanol (80 mL) at room temperature. The mixture was evaporated to dryness under reduced pressure. The residue was dissolved in water (80 mL) and saturated with sodium carbonate. The aqueous layer was exacted with ethyl acetate (40 mL) by three times. The combined organic layers were dried by magnesium sulfate anhydrous and evaporated to give **compound 2** as a yellow loil. Yield (9.33 g), percentage yield (54 %). IR/cm^{-1}: 3349, 2980, 2929, 1693, 1529, 1450, 1360, 1250, 1172, 864. ^{1}H NMR ($CDCl_3$, 400MHz, δ/ppm): 4.71 (s, 1H, -NH-), 3.06 (t, 2H, -$NHCH_2$-), 2.63 (t, 2H, -CH_2- close to amino), 1.64 (s, 2H, -NH_2), 1.00-1.50 (s, 17H, -CH_3,-CH_2-). ESI-MS (m/z): 216. Found: 217 $[M+H]^+$. Analysis calcd. For $C_{11}H_{24}N_2O_2$, C: 61.11, H: 11.11, N: 12.96. Found: C: 61.15, H: 11.14, N: 13.03. [See SI-Fig.4-6]

3.3 Synthesis of SWNTs 3 and SWNTs 4

To a suspension of **SWNTs-COOH** (100 mg) in dry dimethyl formamide (DMF) (20 mL) which was sonicated in an ultrasonic washer for 30 min were added *N*-(3-dimethylaminopropyl)-*N′*-ethylcarbodiimide hydrochloride (EDC·HCl) (100 mg), 1-hydroxy-benzotriazole (HOBt) (100 mg) and **compound 1** (0.25 g). The mixture was stirred at room temperature under nitrogen for 36 h. The solution was filtered and the black solid was washed with DMF, dichloromethane (CH_2Cl_2) and diethyl ether affording functionalized **SWNTs 3**. Instead of **compound 1** we used **compound 2** (0.42 g) and the same reaction procedure to obtain **SWNTs 4**.

3.4 Synthesis of SWNTs 5 and SWNTs 6

To a suspension of **SWNTs 3** (10 mg) in dry CH_2Cl_2 (5 mL) which was sonicated for 30 min was added trifluoroacetic acid (TFA) (1 mL). The reaction mixture was stirred at room temperature under nitrogen for 2 h. The solution was filtered and the black solid was washed with CH_2Cl_2 and dry ethanol affording functionalized **SWNTs 5**. The same reaction procedure leads to obtain **SWNTs 6**.

3.5 Synthesis of DZnPc 7

Tetra-[3,5-*di*-(4-cyanobenzyloxy)benzyloxy] zinc (II) phthalocyanine was synthesized by condensation of 3,5-*di*-(4-cyanobenzyloxy)benzyloxy phthalonitrile in the presence of acetate zinc in 60% yield [20]. The *tetra*-[3,5-*di*-(4-carboxylicbenzyloxy)benzyloxy] zinc (II) phthalocyanine **DZnPc 7** was obtained by hydrolyzed *tetra*-[3,5-*di*-(4-cyanobenzyloxy)benzyloxy] zinc (II) phthalocyanine (0.50 g, 0.2mmol) in NaOH as a green solid[21]. Yield (0.36 g), percentage yield (82%). IR/cm^{-1}: 3300, 2930, 1690, 1600, 1450, 1430, 1318, 1295, 1250, 1153, 1067, 1020, 822, 580; ^{1}H NMR (DMSO-d_6, 400MHz, δ/ppm): 7.90-7.92 (d, *J*=8Hz, 16H, HOOCPh-H), 7.50-7.52 (d, *J*=8Hz, 16H, HOOCPh-H), 7.18 (s, 4H, Pc-H), 7.04-7.06 (d, *J*=8Hz,4H, Pc-H), 6.92-6.93 (d, *J*=4Hz, 4H, Pc-H), 6.71 (s, 4H, Ar-H),6.55 (s, 4H, Ar-H), 5.23 (s, 4H, $PhCH_2O$), 5.14 (s, 4H, $PhCH_2O$), 5.08 (s, 4H, $PhCH_2O$). MALDI-TOF-MS (m/z): 2201. Found: 2203 [M+2]$^+$.Analysis Calcd. For $C_{124}N_8H_{88}O_{28}Zn$ (%): C: 70.02, H: 4.14, N: 5.27. Found: C: 70.01, H: 4.16, N: 5.29. (See SI-Fig.7-9)

3.6 Synthesis of SWNTs-E-DZnPc 8 and SWNTs-H-DZnPc 9

To a suspension of **SWNTs 5** (10 mg) in anhydrous DMF (20 mL) which was sonicated for 30 min were added EDC·HCl (100 mg), HOBt (100 mg) and the dendritic phthalocyanine **DZnPc 7** (20 mg) were added. The reaction mixture was continuously stirred at room temperature under nitrogen for 36 h. The solution was filtered and the black solid was washed with CH_2Cl_2 and anhydrous ethanol affording **SWNTs-E-DZnPc 8**. According to the above procedure, **SWNTs 6** (10 mg) was treated with EDC·HCl

(100 mg), HOBt (100 mg) and the dendritic phthalocyanine **DZnPc 7** (20 mg) to give **SWNTs-H-DZnPc 9**. The structures of **SWNTs 5, SWNTs 6, SWNTs-E-DZnPc 8** and **SWNTs-H-DZnPc 9** were characterized by IR, Raman spectroscopy, transmission electron microscopy and thermal gravimetric analysis methods which would be discussed in the following chapter.

4. Results and discussion

The synthetic route for the dendritic phthalocyanine-single-wall carbon nanotube nanoconjugates was shown in scheme **1**.

4.1 Synthesis and characterization

The carbodiimide-active amidation reaction was used to functionalize the surface bound carboxylic acid groups the SWNTs (**SWNTs-COOH**) with a functional dendritic phthalocyanine **DZnPc 7** using either ethylenediamine or hexamethylenediamine as a spacer linker in DMF. In brief, **compound 1** was firstly obtained by reaction of ethylenediamine with 2 equivalents of *di*-*tert*-butyl dicarbonate. Then, **SWNTs 3** with Boc protecting groups were obtained by reaction of **SWNTs-COOH** with EDC·HCl, HOBt and **compound 1** in DMF. After that, the Boc protecting groups of **SWNTs 3** were removed by using 25-50% TFA in CH_2Cl_2 affording **SWNTs 5** with amine groups. The dendritic phthalocyanine **DZnPc 7** was successfully synthesized via a convergent approach. Its structure was unambiguously characterized by means of elemental analysis, IR, MALDI-TOF-MS and ^{1}H NMR [20]. Finally, the coupling reaction between the amine groups of **SWNTs 5** and the carboxylic groups of the dendritic phthalocyanine **DZnPc 7** in the presence of EDC·HCl and HOBt gave a nanoconjugate **SWNTs-E-DZnPc 8** with ethylenediamine as the spacer linker through amidation reaction. The similar synthetic procedure was carried out to obtain a nanoconjugate **SWNTs-H-DZnPc 9** with hexamethylenediamine as the spacer linker. The constitutions, structures and morphologies of

SWNTs-E-DZnPc 8 and **SWNTs-H-DZnPc 9** were characterized by combination of analytical techniques, such as IR, Raman spectroscopy, transmission electron microscopy (TEM) and thermal gravimetric analysis (TGA).

The morphologies of the **SWNTs-COOH**, **SWNTs-E-DZnPc 8** and **SWNTs-H-DZnPc 9** were studied by TEM. The images of **SWNTs-COOH**, **SWNTs-E-DZnPc8** and **SWNTs-H-DZnPc9** are shown in Figure 1. The image of pristine **SWNTs-COOH** showed a clean sidewall with a diameter of about 20 nm (Fig.1 (a)). The black spots originated from the dendritic phthalocyanine indicated by white circles on the SWNTs, evidence of the existence of the dendritic phthalocyanine on the **SWNTs-E-DZnPc 8** and **SWNTs-H-DZnPc 9** with diameters of about 23 and 24 nm, respectively (Fig.1 (b) and Fig.1 (c).

Further evidence to support covalent functionalization of SWNTs was found in the IR spectra. Figure 2 showed the IR spectra of **SWNTs-COOH**, **SWNTs-E-DZnPc 8**, **SWNTs-H-DZnPc 9** and **DZnPc 7**. A symmetrical C=O stretching at 1733 cm^{-1} was assigned to the vibration of COOH moieties of **SWNTs-COOH**. **SWNTs-E-DZnPc 8**, **SWNTs-H-DZnPc 9** both displayed band at 1720 cm^{-1}, which was matched with the vibration of the amide functional groups after the COOH moieties of SWNTs being reacted with either ethylenediamine or hexamethylenediamine [22]. Finally, the IR spectra of **SWNTs-E-DZnPc 8** and **SWNTs-H-DZnPc 9** also displayed other bands that were coincident with those displayed by **DZnPc 7**.

Raman spectroscopy provided essential and useful information that the dendritic phthalocyanines have been successful covalently attached to the carbon nanotube sidewalls. Raman spectra of the nanoconjugates were shown in Figure 3. There were two principal bands at about 1330-1380 cm^{-1} (D band) and 1400-1600 cm^{-1} (G band). The former was used to indicate the density of the defects for the

SWNTs and had been used to monitor the process of covalent functionalization which transformed from sp^2 to sp^3 site; while the latter could be used to estimate the level and distribution of modification [23]. Upon excitation at 785 nm, the intensity of **SWNTs-E-DZnPc 8** and **SWNTs-H-DZnPc 9** at 1386 cm^{-1} was stronger than that of the pristine **SWNTs-COOH**, which suggests a significant modification after the addition of phthalocyanine via a covalent bond [24-25]. Besides, some new features located at 682 and 749 cm^{-1} for **SWNTs-E-DZnPc 8** and **SWNTs-H-DZnPc 9** were assigned to the δ vibration of macromolecular zinc phthalocyanine, which can be clearly observed in Fig.3 [26]. The above results confirmed the presence of zinc phthalocyanine particles on the SWNTs. Furthermore, radial breathing modes (RBMs) were very sensitive to diameter and structure of the nanotubes. The RBM bands were observed between 166 and 266 cm^{-1} for the all compounds. The peaks at 266 and 166 cm^{-1} were hardly discernible for the pristine SWNTs, but obviously observed for the functionalized SWNTs. This result implied that the nanoconjugates were enriched on the nanotubes with slightly larger diameters after reaction.

The amounts of dendritic phthalocyanine covalently linked with the SWNTs were determined by TGA. Figure 4 showed the thermal decomposition profiles of **SWNTs-COOH**, **DZnPc 7**, **SWNTs-E-DZnPc 8** and **SWNTs-H-DZnPc 9**. **SWNTs-COOH, SWNTs-E-DZnPc 8** and **SWNTs-H-DZnPc 9** presented a loss of weight about 8.9 %, 21 % and 32 %, respectively, at 650°C. The initial mass loss for each sample before 200°C may be attributed to the solvent loss, therefore the corrected weight losses due to the functional groups on nanotubes were then estimated to be 12 % for **SWNTs-E-DZnPc 8**, 23 % for **SWNTs-H-DZnPc 9** and 50 % for **DZnPc 7**. A simple calculation permitted a loss of weight of 28% to be estimated if all carboxylic groups of the SWNTs-COOH (the content of -COOH: 2.73%) were functionalized by the dendritic phthalocyanine. So a weight loss at about 12 % and 23 % indicated that not all carboxylic groups on the SWNTs have been reacted. This result corresponds with the calculated result that one dendritic zinc phthalocyanine for about 614 and 1345 carbon atom for **SWNTs-E-DZnPc 8** and **SWNTs-H-DZnPc 9** [27].

4.2 Photophysical properties

The UV/Vis absorption spectra of **SWNTs-COOH**, **DZnPc 7**, **SWNTs-E-DZnPc 8** and **SWNTs-H-DZnPc 9** were shown in Figure 5. The dendritic phthalocyanine **DZnPc 7** showed a B-band at 350 nm and a Q-band at about 685 nm. Additionally, there is a UV band at 290 nm, which can be assigned to dendritic substituent chromophores. The van Hove singularities of SWNTs [28]were observed through the recorded range between 300 and 800 nm. The UV/Vis absorption spectra of **SWNTs-E-DZnPc 8** and **SWNTs-H-DZnPc 9** nanoconjugates provided unquestionable evidence for the existence of both constituents: SWNTs and dendritic phthalocyanines. Therefore, the electronic structure of the SWNTs was largely preserved.

Figure 6 showed the fluorescence spectra of **DZnPc 7**, **SWNTs-E-DZnPc 8** and **SWNTs-H-DZnPc 9** in DMF. Upon excitation at 610 nm, **DZnPc 7** exhibited fluorescence emissions at 708 nm, with the fluorescence quantum yield of 0.10 which was calculated according to eq.1 [29] and lifetime (τ) of 2.92 ± 0.29 ns. While the **SWNTs-E-DZnPc 8** and **SWNTs-H-DZnPc 9** exhibited about 98% and 97% quenching of the phthlocyanine's emission at 715 and 750 nm, respectively. Excitation at different wavelength (350, 610 nm) also showed a similar quenching for the emission of phthalocyanines (See SI-Fig.10-13), supporting the presence of an electron-transfer process from the dendritic phthalocyanine to the carbon nanotubes through the spacer linker. The intensity of the emission bands increased with the addition of an equimolar amount of free dendritic phthalocyanine into the solution of **SWNTs-E-DZnPc 8** and **SWNTs-H-DZnPc 9** (See SI-Fig.14-15), further evidenced the fact that intramolecular electron transfer did occur between dendritic phthalocyanine (electron donor) and the carbon nanotubes (electron acceptor) during a photoinduced process.

$$\Phi_x = \Phi_{ZnPc} \times \frac{F_x}{F_{ZnPc}} \times \frac{A_{ZnPc}}{A_x} \qquad \text{eq.1}$$

Where Φ_{ZnPc} is the fluorescence quantum yield of **ZnPc** in DMF, F_x is the fluorescence of integral of either **SWNTs-E-DZnPc 8** or **SWNTs-H-DZnPc 9**, F_{ZnPc} is the fluorescence of integral of **ZnPc**, A_{ZnPc} is the absorbance of **ZnPc** and A_x is the absorbance of either **SWNTs-E-DZnPc 8** or **SWNTs-H-DZnPc 9**.

The fluorescence lifetimes (τ) of the **SWNTs-E-DZnPc 8**, **SWNTs-H-DZnPc 9** and **DZnPc 7** were studied by time-resolved spectroscopy. The fluorescence decay curves of **SWNTs-E-DZnPc 8**, **SWNTs-H-DZnPc 9** and **DZnPc 7** were shown in Figure 7. The fluorescence lifetimes were found to fit a mono-exponential function: $f(t) = A + B_1e^{-t/\tau_1} + B_2e^{-t/\tau_2}$. The fitting data was summarized in Table 1. The fluorescence lifetimes (τ) of the **SWNTs-E-DZnPc 8** and **SWNTs-H-DZnPc 9** were 2.53 ± 0.25 ns and 2.62 ± 0.26 ns, respectively, bearing resemblance to that of the free **DZnPc 7**, which has a lifetime of 2.92 ± 0.29 ns. A possible rational explanation was that the dendritic phthalocyanine chromophores didn't interact with the SWNTs, due to the dendritic structure. Meanwhile, the slight difference in lifetimes between the **SWNTs-E-DZnPc 8** and **SWNTs-H-DZnPc 9** can be ascribed to the spacer linker length. It implied that quicker the electronic exchange between the dendritic phthalocyanine and SWNTs would occur by shortening the spacer linker. The length of spacer linker between the dendritic phthalocyanine and SWNTs also exerted an effect on the photoinduced intramolecular electron transfer efficiency (Φ_{SET}) and electron transfer rate constant (K_{SET}) of the nanoconjugates. The values of Φ_{SET} and K_{SET} calculated by eqs.2-3 were shown in Table 1. The Φ_{SET} and K_{SET} of **SWNTs-E-DZnPc 8** with ethylenediamine showed higher fluorescence quenching efficacy and larger electron transfer rate constant than that of the **SWNTs-H-DZnPc 9**. This result further confirmed that the larger electronic exchange rate and the higher electronic transfer efficiency between dendritic phthalocyanine and SWNTs were observed with decreasing the length of spacer linker.

$$\Phi_{\mathrm{SET}} = 1 - \tau_{SWNTs\text{-}E\text{-}DZnPc8 \text{ or } SWNTs\text{-}H\text{-}DZnPc9} / \tau_{DZnPc7} \qquad \text{eq.2}$$

$$\mathrm{K}_{\mathrm{SET}} = 1/\tau_{SWNTs\text{-}E\text{-}DZnPc8 \text{ or } SWNTs\text{-}H\text{-}DZnPc9} - 1/\tau_{DZnPc7} \qquad \text{eq.3}$$

Where $\tau_{\textbf{SWNTs-E-DZnPc 8} \text{ or } \textbf{SWNTs-H-DZnPc 9}}$ is the fluorescence lifetime of either **SWNTs-E-DZnPc 8** or **SWNTs-H-DZnPc 9**, while $\tau_{\textbf{DZnPc 7}}$ is the fluorescence lifetime of **DZnPc 7**.

5 Conclusions

A novel series of dendritic phthalocyanine-single-wall carbon nanotube nanoconjugates, zinc (II) phthalocyanine bearing poly (aryl benzyl ether) dendritic substituents covalently linked with SWNTs through either ethylenediamine or hexamethylenediamine as the spacer linker, were synthesized and characterized. These nanoconjugates exhibited quenching of the fluorescent emission at the Q-band of the phthalocyanine upon excitation at 610 nm, which is due to a photoinduced intramolecular electron transfer between the dendritc phthalocyanine and SWNTs through the spacer linker. The length of spacer linker between the dendritic phthalocyanine and SWNTs had a marked influence on intramolecular electron transfer efficiency and electron rate constant. The shorter the spacer linker, the quicker the electron exchange constant and the higher electron transfer efficiency between the dendritic phthalocyanine and SWNTs were observed. This study suggested that dendritic phthalocyanine-single-wall carbon nanotube nanoconjugates may find potential application as biological labels.

Acknowledgement

This research was supported by the National Natural Science Foundation of China (21274021, 20604007); Natural Science Foundation of Fujian, China (2011J01029) and the Science Research Foundation of Ministry of Health, China (WKJ2008-2-61) and Fujian Normal University's student innovation programme(Sjcxcy-2012004).

References

[1] Sinnott SB and Andrews R. Carbon Nanotubes: Synthesis, properties, and applications. Crit Rev Solid State Mater 2001; 26: 145-72.

[2] Odom TW, Huang JL, Kim P and Lieber CM. Structure and electronic properties of carbon nanotubes. J Phys Chem B 2000; 104: 2794-1.

[3] Li J, Wang YB, Qiu JD, Sun DC and Xia XH. Biocomposites of covalently linked glucose oxidase on carbon nanotubes for glucose biosensor. Anal Bioanal Chem 2005; 383: 918-2.

[4] Guldi DM, Rahman GMA, Prato M, Jux N, Quin S and Ford W. Single-wall carbon nanotubes as integrative building blocks for solar-energy conversion. Angew Chem Int Ed 2005; 117: 2015-1.

[5] Guldi DM, Rahman GMA, Quin S, Tchoul M, Ford WT, Marcaccio M, et al. Versatile coordination chemistry towards multifunctional carbon nanotube nanohybrids. Chem-Eur J 2006; 12: 2152-1.

[6] Baskaran D, Mays JW, Zhang XP and Bratcher MS. Carbon nanotubes with covalently linked porphyrin antennae: photoinduced electron transfer. J Am Chem Soc 2005; 127: 6916-1.

[7] Alvaro M, Atienzar P, de la Cruz P, Delgado JL, Troiani V, Garcı´a H, et al. Synthesis, photochemistry, and electrochemistry of single-wall carbon nanotubes with pendent pyridyl groups and of their metal complexes with zinc porphyrin. comparison with pyridyl-bearing fullerenes. J Am Chem Soc 2006; 128: 6626-1.

[8] Tanaka H, Yajima T, Matsumoto T, Otsuka Y and Ogawa T. Porphyrin molecular nanodevices wired using single-walled carbon nanotubes. Adv Mater 2006; 18: 1411-1.

[9] Ehli C, Rahman GMA, Jux N, Balbinot B, Guldi DM, Paolucci F, et al. Interactions in single-wall carbon nanotubes/pyrene/porphyrin nanohybrids. J Am Chem Soc 2006; 128: 11222-1.

[10] Guldi DM, Marcaccio M, Paolucci D, Paolucci F, Tagmatarchis N, Tasis D, et al. Single-wall carbon nanotube-ferrocene nanohybrids: observing intramolecular electron transfer in functionalized SWNTs. Angew Chem Int Ed 2003; 115: 4338-1.

[11] Martin RB, Qu LW, Lin Y, Harruff BA, Bunker CE, Sun YP, et al. Functionalized carbon nanotubes with tethered pyrenes: synthesis and photophysical properties. J Phys Chem B 2004; 108: 11447-1

[12] Ballesteros B, Torre GDL, Ehli C, Rahman GMA And Torres TJ. Single-wall carbon nanotubes bearing covalently linked phthalocyanines-photoinduced electron transfer. J Am Chem Soc 2007; 129: 5061-4.

[13] Zhang MF, Murakami T, Ajima K, Tsuchida K, Sandanayaka ASD, et al. Fabrication of ZnPc/protein nanohorns for double photodynamic and hyperthermic cancer phototherapy. Proc Natl Acad Sci USA 2008; 105: 14773-2.

[14] Ballesteros B, Campidelli S, Torre GDL, Ehli C, Guldi DM, Prato M, et al. Synthesis, characterization and photophysical properties of a SWNT phthalocyanine hybrid. Chem Commun 2007; 28: 2950-2.

[15] Campidelli S, Ballesteros B, Filoramo A, Dı´az DD, Torre GDL, Torres T, et al. Facile decoration of functionalized single-wall carbon nanotubes with phthalocyanines via “click chemistry”. J Am Chem Soc 2008; 130: 11503-5.

[16] Bartelmess J, Ballesteros B, Torre GDL, Kiessling D, Campidelli S, Prato M, et al. Phthalocyanine-pyrene conjugates: a powerful approach toward carbon nanotube solar cells. J Am Chem Soc 2010; 132: 16202-4.

[17] Chidawanyika W and Nyokong T. Characterization of amine-functionalized single-walled carbon nanotube-low symmetry phthalocyanine conjugates. Carbon 2010; 48: 2831-6.

[18] Saari WS, Schwering JE, Lyle PA, Smith SJ and Engelhardt EL. Cyclization-activated prodrugs. basic carbamates of 4-hydroxyanisole. J Med Chem 1990; 33: 97-4.

[19] Ravikumar VT. A Convenient Large Scale Synthesis Of N-Boc-ethylenediamine. Synthetic Commun 1994; 24: 1767-2.

[20] Peng YR, Zhang H, Wu HL, Huang BQ, Gan L and Chen Z. The synthesis and photophysical properties of zinc (II) phthalocyanine bearing poly (aryl benzyl ether) dendritic substituents. Dyes Pigm 2010; 87: 10-4.

[21] He DD, Zhang H, Peng YR, Ma DD, Wang YH, Yang HQ, et al. Synthesis and characterization of a novel frétchet dendritic phthalocyanine zinc (II): Tetra-{3,5-di-[3,5-di(4-carboxylic benzyloxy) benzyloxy] benzyloxy} Phthalocyanine Zinc(II). Chin J Org Chem 2012; 32: 1321-6.

[22] Yang ZL, Chen HZ, Cao L, Li HY, Wang M. Synthesis and photoconductivity study of carbon nanotube bonded by tetrasubstituted amino manganese phthalocyanine. Mater Sci Eng. B 2004; 106: 73-2.

[23] Bahr JL, Yang JP, Kosynkin DV, Bronikowski MJ, Smalley RE, and Tour JM. Functionalization of carbon nanotubes by electrochemical reduction of aryl diazonium salts: a bucky paper electrode. J Am Chem Soc 2001; 123: 6536-3.

[24] Dillon EP, Crouse CA and Barron AR. Synthesis, characterization, and carbon dioxide adsorption of covalently attached polyethyleneimine-functionalized single-wall carbon nanotubes. Acs Nano 2008; 2: 156-5.

[25] Dresselhaus MS, Dresselhaus G and Jorio A. Raman spectroscopy of carbon nanotubes in 1997 and 2007. J Phys Chem C 2007; 111: 17887-1.

[26] Khanh HLH, Rivier L, Jousselme B, Jegou P, Filoramo A and Campidelli S. Zn-porphyrin /zn-phthalocyanine dendron for SWNT functionalisation. Chem Commun 2010; 46: 8731-2.

[27] Campidelli S, Ballesteros B, Filoramo A, Dı´az DD, Torre GDL, Torres T, et al. Facile decoration of functionalized single-wall carbon nanotubes with phthalocyanines via "click chemistry". J Am Chem Soc 2008; 130: 11503-4.

[28] Campidelli S, Sooambar C, Diz EL, Ehli C, Guldi DM and Prato M. Dendrimer-functionalized single-wall carbon nanotubes: synthesis, characterization, and photoinduced electron transfer. J Am Chem Soc 2006; 128: 12544-6.

[29] Fery-Forgues S and Lavabre D. Are fluorescence quantum yields so tricky to measure? A demonstration using familiar stationery products. J Chem Educ 1999; 76: 1260-1.

Figure 1 TEM images of SWNTs-COOH (a), SWNTs-E-DZnPc8 (b) and SWNTs-H-DZnPc9 (c)

Figure 2 IR spectra of SWNTs-COOH, DZnPc7, SWNTs-E-DZnPc8 and SWNTs-H-DZnPc9

Figure 3 Raman Spectra of SWNTs-COOH, DZnPc7, SWNTs-E-DZnPc8 and SWNTs-H-DZnPc9

Figure 4 TGA curves of SWNTs-COOH, DZnPc7, SWNTs-E-DZnPc8 and SWNTs-H-DZnPc9

Figure 5 UV/Vis of SWNTs-COOH, DZnPc7, SWNTs-E-DZnPc8 and SWNTs-H-DZnPc9 in DMF at room temperature ($C_{\text{SWNTs-COOH, DZnPc7, SWNTs-E-DZnPc8 and SWNTs-H-DZnPc9}} = 2\times10^{-5}$ mol/L)

Figure 6 Steady-state fluorescence spectra of DZnPc7, SWNTs-E-DZnPc8 and SWNTs-H-DZnPc9 in DMF at room temperature (λ_{ex} = 610 nm). Curves for SWNTs-E-DZnPc8 and SWNTs-H-DZnPc9 have been amplified by a factor of 20. ($C_{\text{DZnPc7, SWNTs-E-DZnPc8 and SWNTs-H-DZnPc9}} = 2\times10^{-5}$ mol/L)

Figure 7 Time-resolved fluorescence spectra of DZnPc7, SWNTs-E-DZnPc8 and SWNTs-H-DZnPc9 in DMF (λ_{ex}= 405 nm, $C_{\text{DZnPc7, SWNTs-E-DZnPc8 and SWNTs-H-DZnPc9}} = 2\times10^{-5}$ mol/L)

Scheme **1** The scheme of synthetic route for dendritic zinc phthalocyanine-SWNTs nanoconjugates

Table 1 Photophysical properties of SWNTs-E-DZnPc8, SWNTs-H-DZnpc9 in DMF

Complexes	Absorption λ_{max}/nm	Emission λ_{max}/nm	Φ_F[a]	τ_s /ns	Φ_{SET}	$K_{SET}(s^{-1})$
DZnPc7	678	709	0.10	2.92	-	-
SWNTs-E-DZnPc8	682	688	0.14	2.53	0.13	5.3×10^7
SWNTs-H-DZnPc9	683	688	0.05	2.62	0.10	3.9×10^7

[a] Znpc（Φ_F=0.30）as the standard.

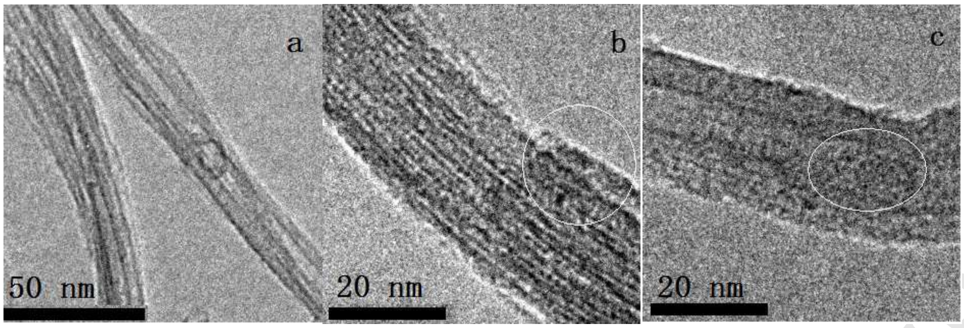

Figure 1

Figure 2

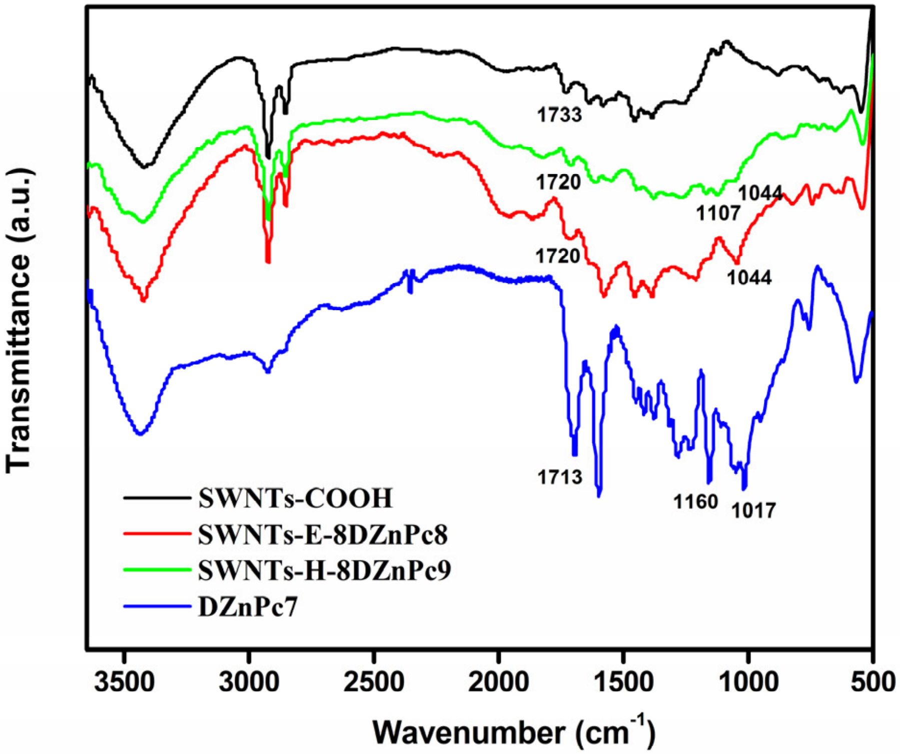
Transmittance (a.u.)
Wavenumber (cm^{-1})
3500
3000
2500
2000
1500
1000
500
1733
1720
1107
1044
1720
1044
1713
1160
1017
SWNTs-COOH
SWNTs-E-8DZnPc8
SWNTs-H-8DZnPc9
DZnPc7

Figure 3

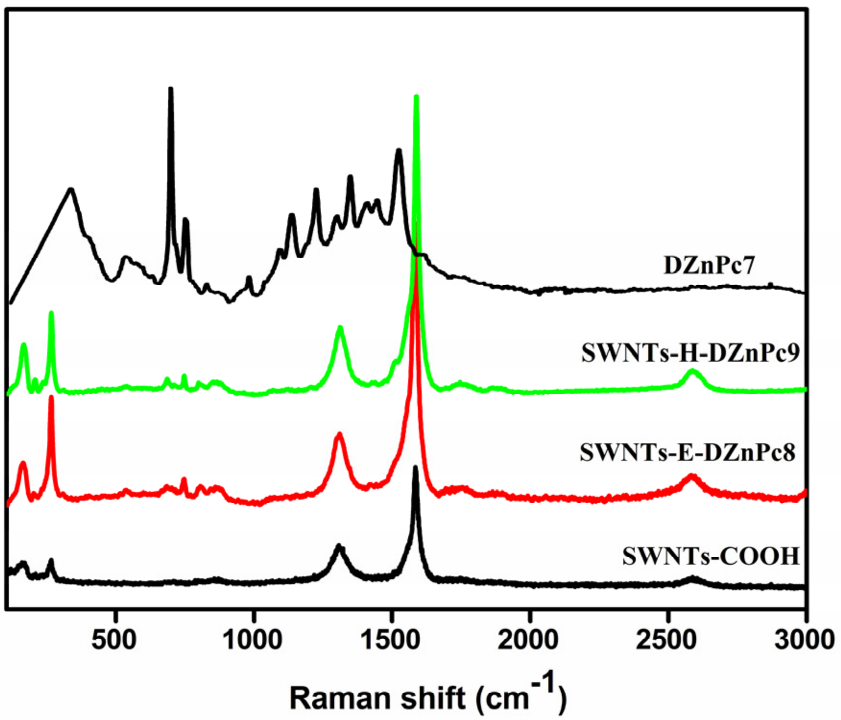
DZnPc7
SWNTs-H-DZnPc9
SWNTs-E-DZnPc8
SWNTs-COOH
500
1000
1500
2000
2500
3000
Raman shift (cm^{-1})

Figure 4

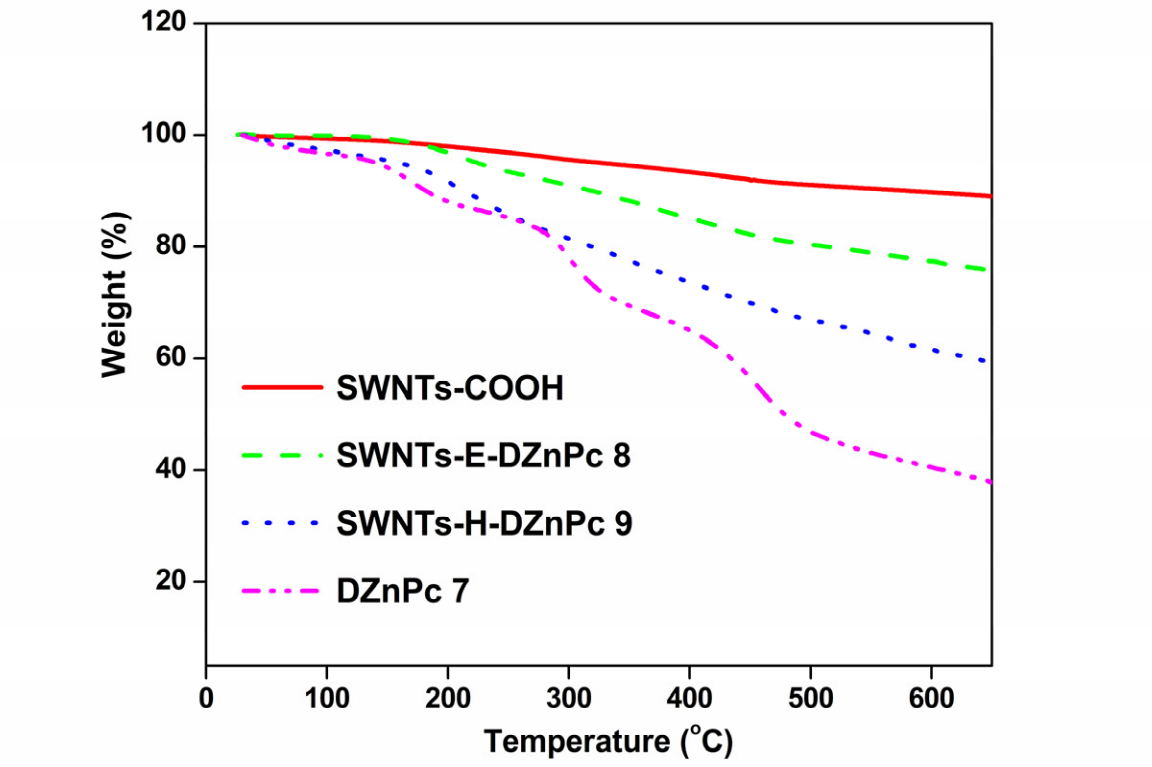

120
100
80
60
40
20
Weight (%)
0
100
200
300
400
500
600
Temperature (°C)
SWNTs-COOH
SWNTs-E-DZnPc 8
SWNTs-H-DZnPc 9
DZnPc 7

Figure 5

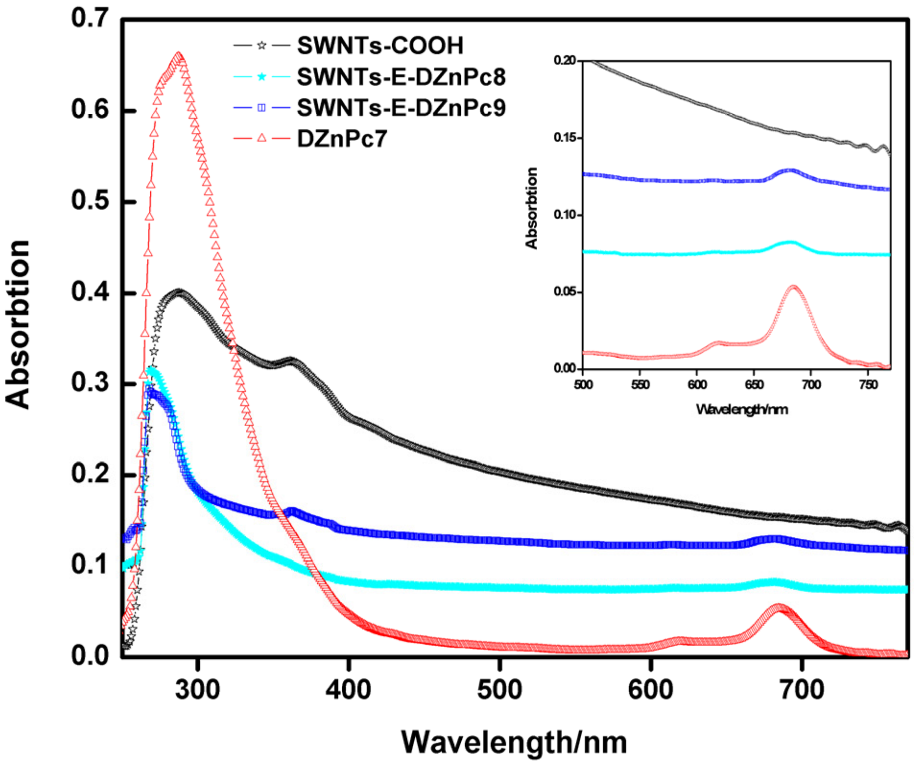
SWNTs-COOH
SWNTs-E-DZnPc8
SWNTs-E-DZnPc9
DZnPc7
Absorbtion
Wavelength/nm
0.0
0.1
0.2
0.3
0.4
0.5
0.6
0.7
300
400
500
600
700
0.00
0.05
0.10
0.15
0.20
500
550
600
650
700
750

Figure 6

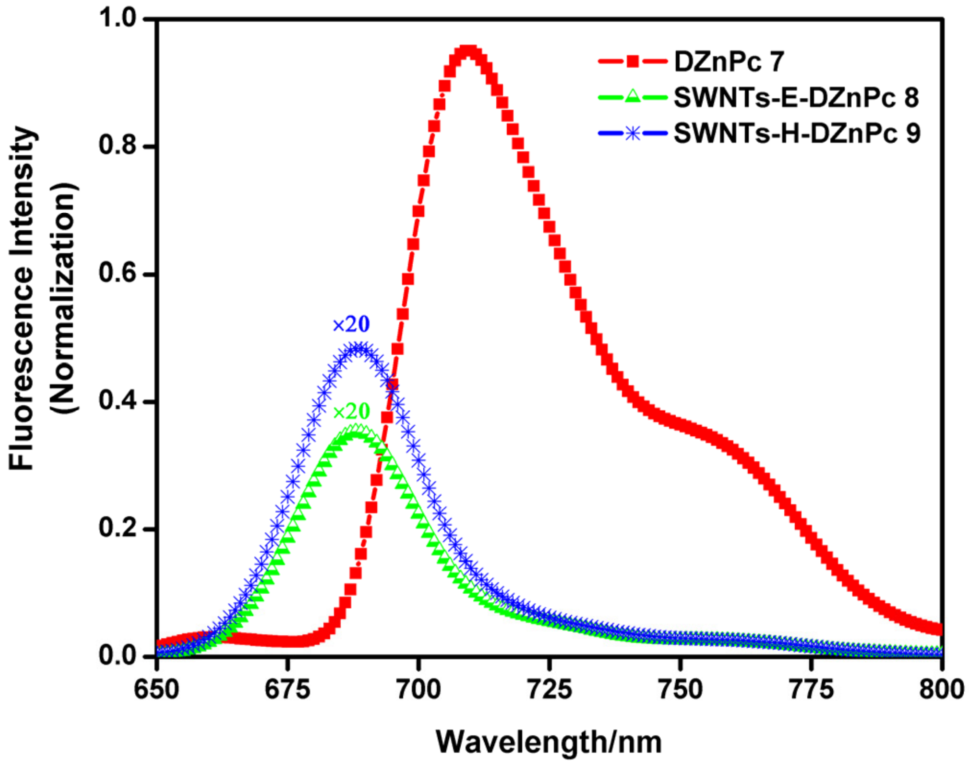
Fluorescence Intensity (Normalization)
Wavelength/nm
1.0
0.8
0.6
0.4
0.2
0.0
650
675
700
725
750
775
800
DZnPc 7
SWNTs-E-DZnPc 8
SWNTs-H-DZnPc 9
×20
×20

Figure 7

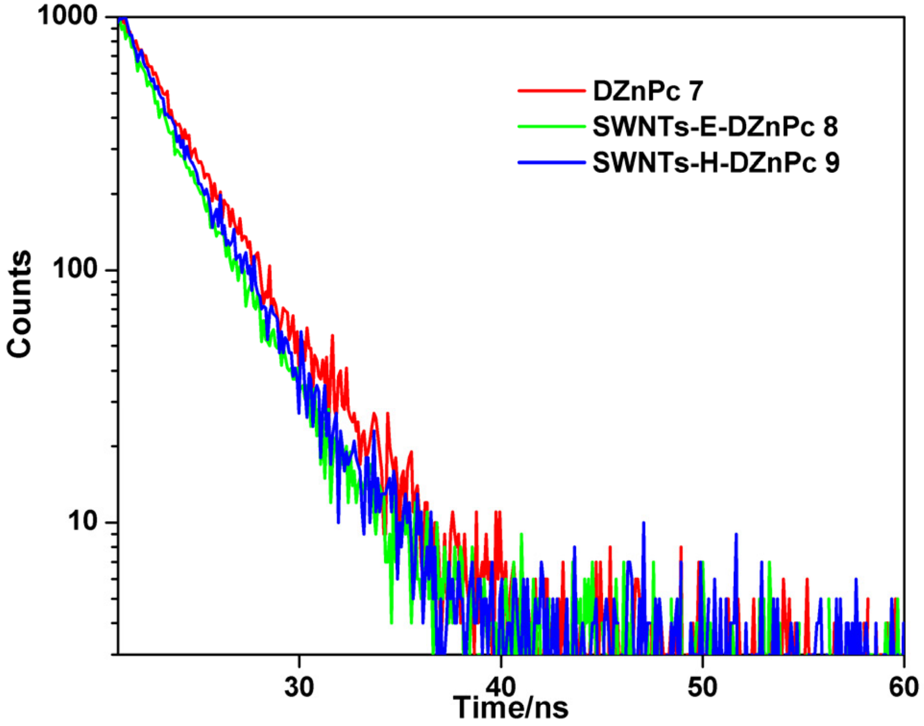
1000
100
10
Counts
30
40
50
60
Time/ns
DZnPc 7
SWNTs-E-DZnPc 8
SWNTs-H-DZnPc 9

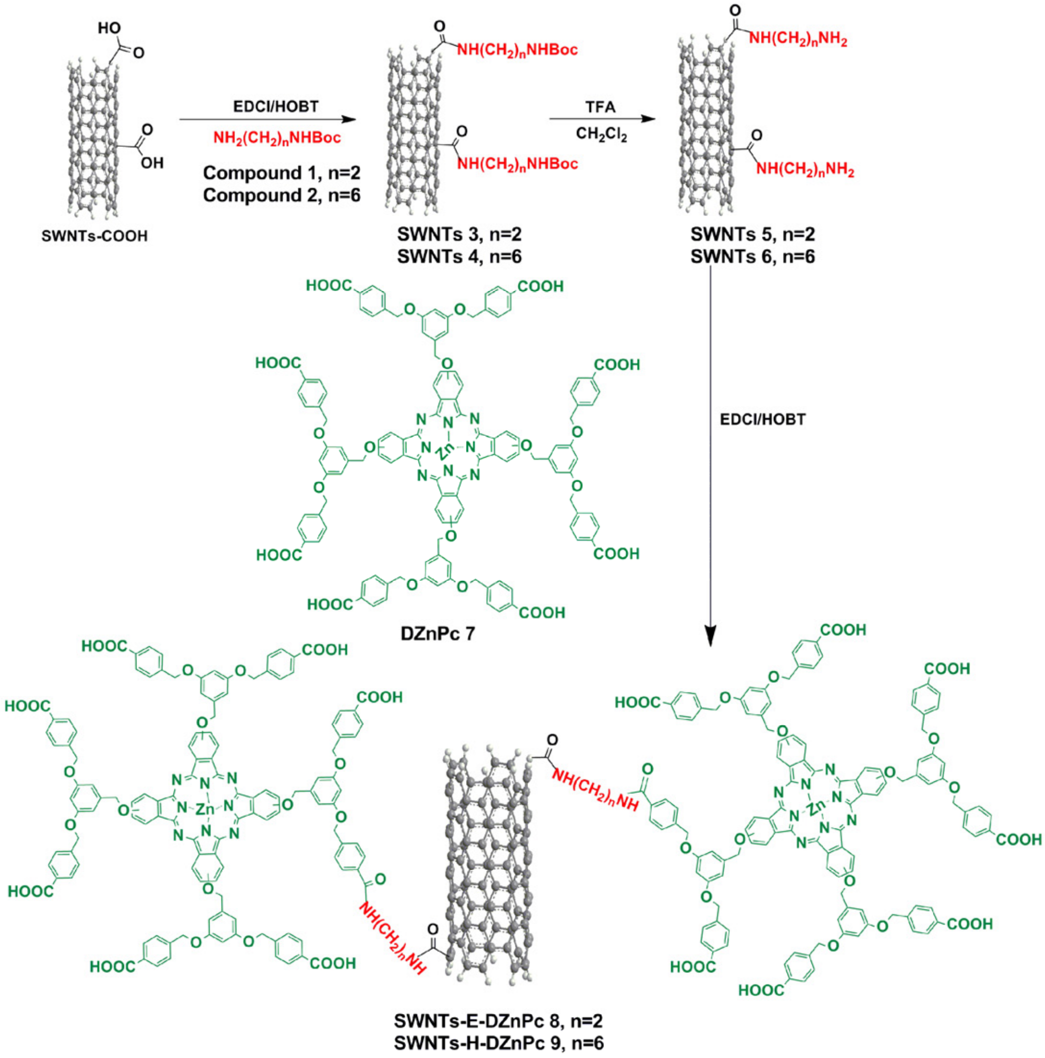
SWNTs-COOH
EDCI/HOBT
NH2(CH2)nNHBoc
Compound 1, n=2
Compound 2, n=6
SWNTs 3, n=2
SWNTs 4, n=6
TFA
CH2Cl2
SWNTs 5, n=2
SWNTs 6, n=6
EDCI/HOBT
DZnPc 7
SWNTs-E-DZnPc 8, n=2
SWNTs-H-DZnPc 9, n=6

Scheme 1

Supporting Information

Single-wall Carbon Nanotubes Covalently Linked with Zinc (□) Phthalocyanine Bearing Poly(aryl benzyl ether) Dendritic Substituents：Synthesis，Characterization and Photoinduced Electron Transfer

Dandan He[1], Yiru Peng[*1], Hongqin Yang[2], Dongdong Ma[1], Yuhua Wang[2]，Kuizhi Chen[1] , Pingping Lin, Kuizhi Chen

[1]College of Chemistry and Engineering, Fujian Provincial Key Laboratory of Polymer Materials, Fujian Normal University, Fuzhou 350007, China
[2]Key Lab of Optoelectronic Science and Technology for Medicine of Ministry of Education, Fujian Normal University, Fuzhou 350007, China

---

[*] Corresponding author. Tel.: + 86 591 8346 5225.
E-mail address: yirupeng@fjnu.edu.cn (Y. Peng).

Experimental

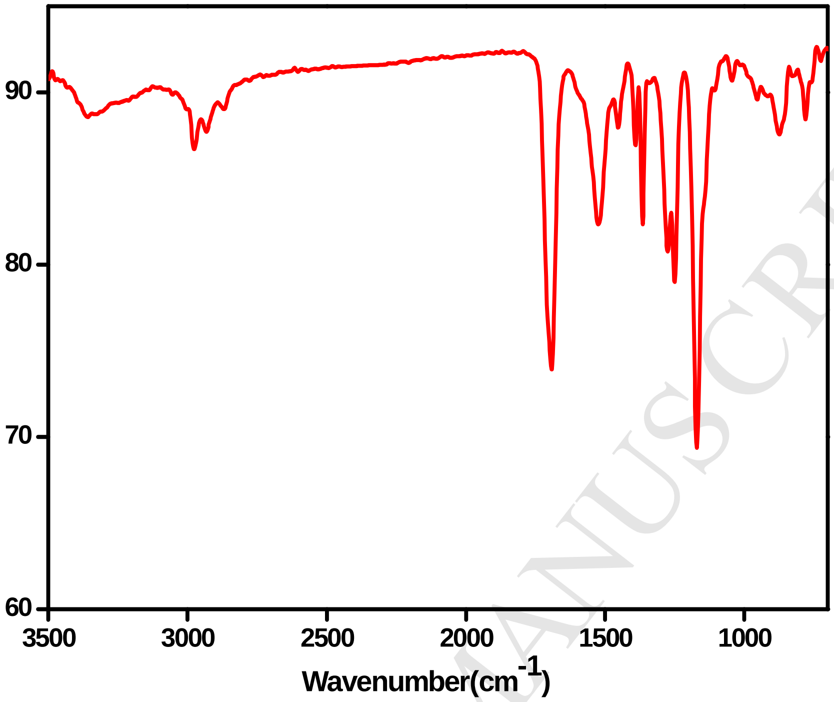

SI-Fig.1 IR spectra of compound 1

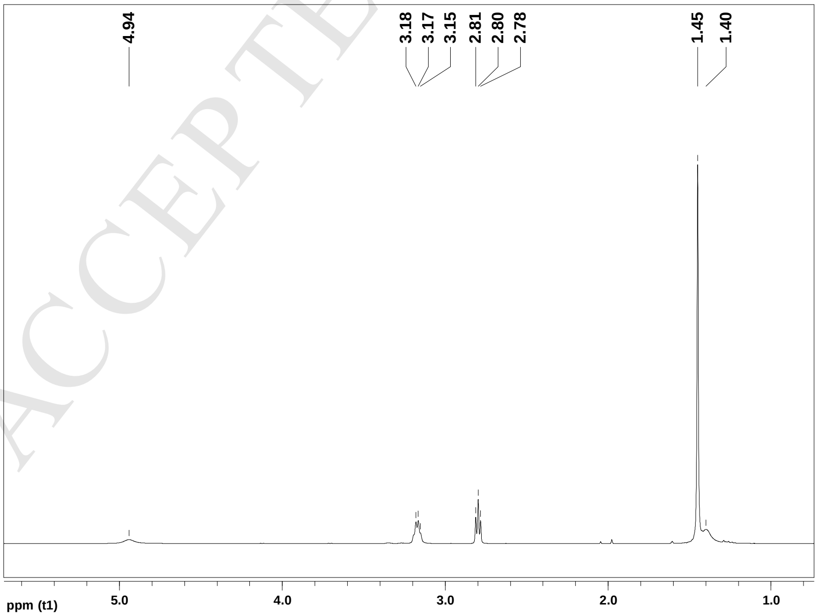

SI-Fig.2 ^{1}H NMR spectra of compound 1

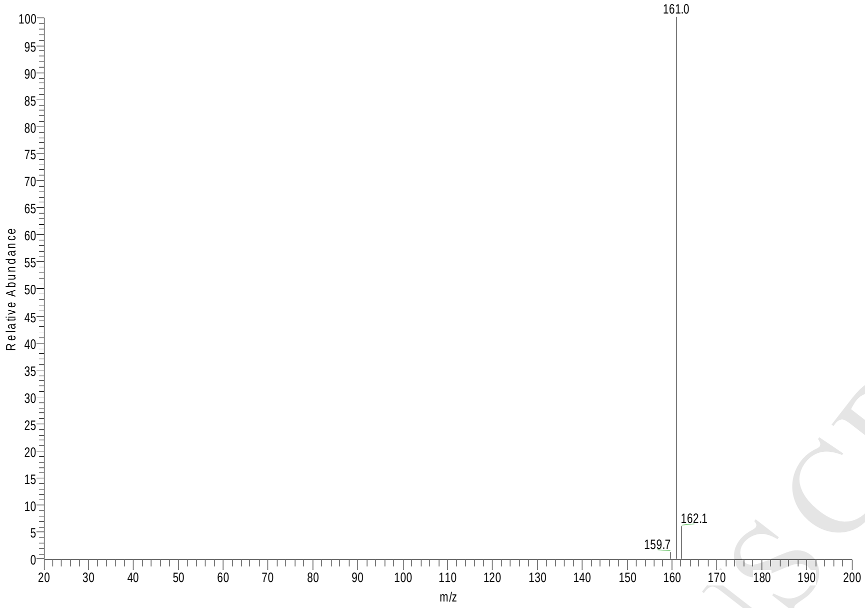

SI-Fig.3 ESI-MS spectra of compound 1

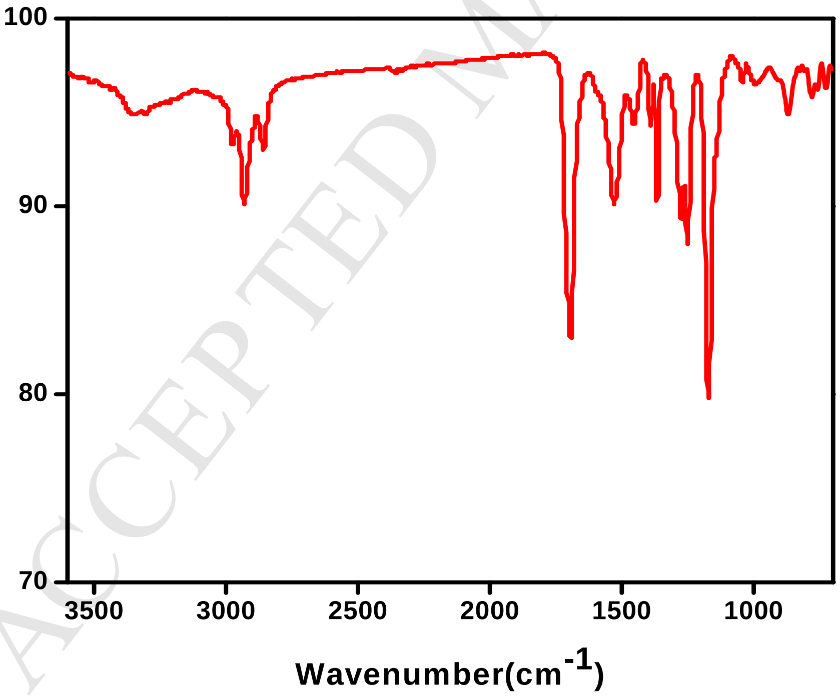

SI-Fig.4 IR spectra of compound 2

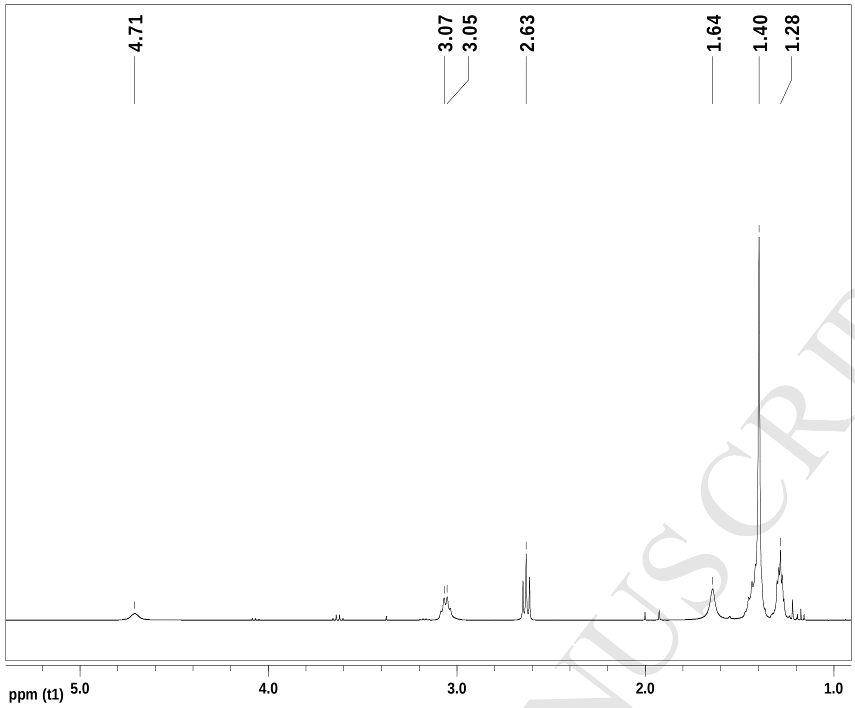

SI-Fig.5 ^{1}H NMR spectra of compound 2

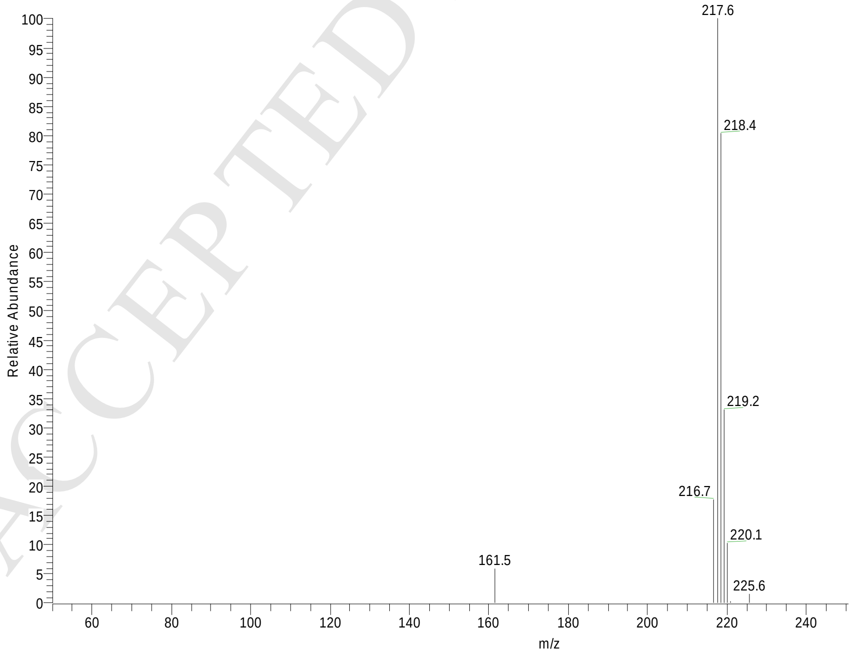

SI-Fig.6 MS spectra of compound 2

Synthesis and characterization

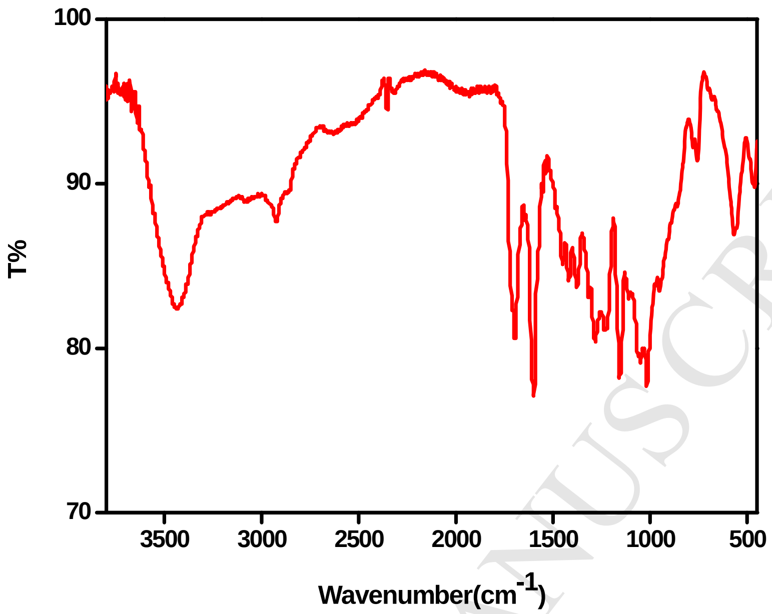

SI-Fig.7 IR spectra of DZnPc7

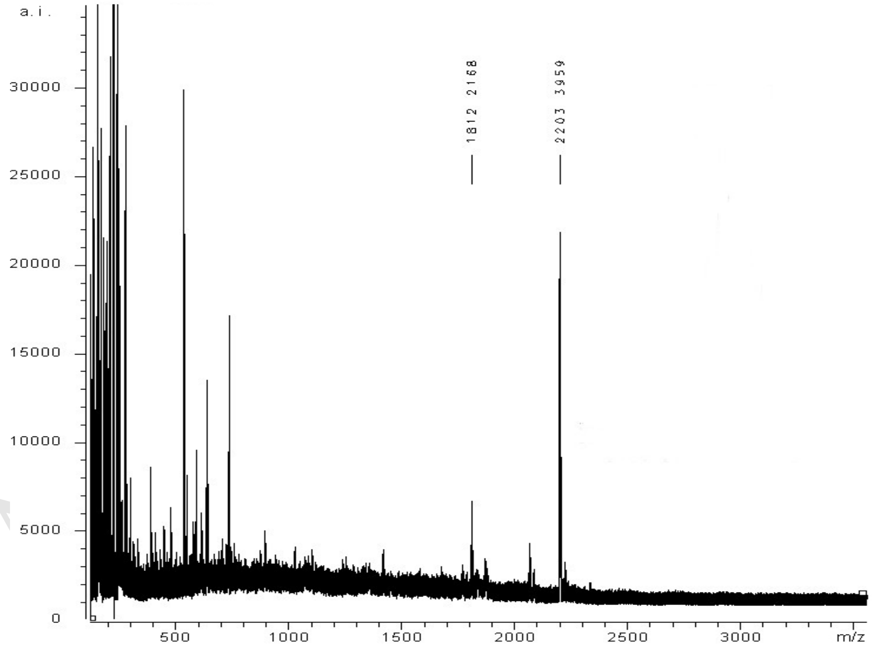

SI-Fig.8 MALDI-TOF-MS spectra of DZnPc7

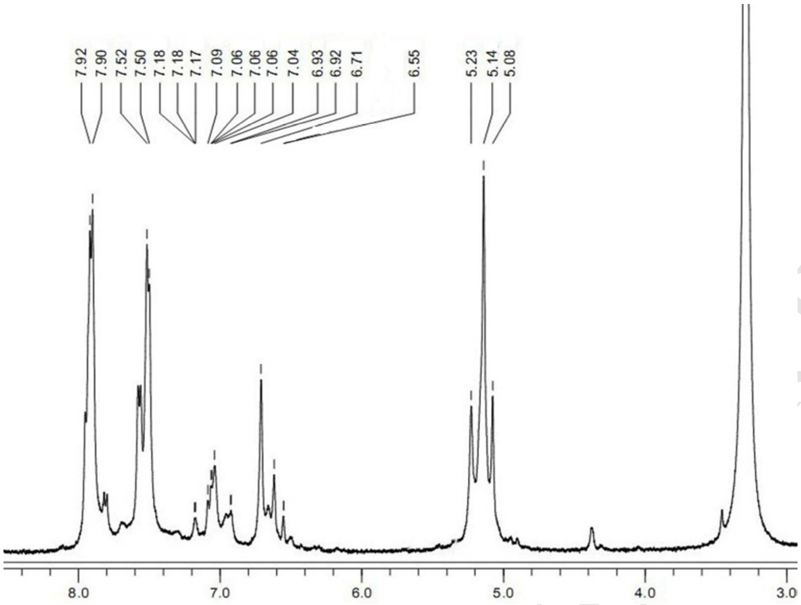

SI-Fig.9 ^{1}H NMR spectra of DZnPc7

Photophysical properties

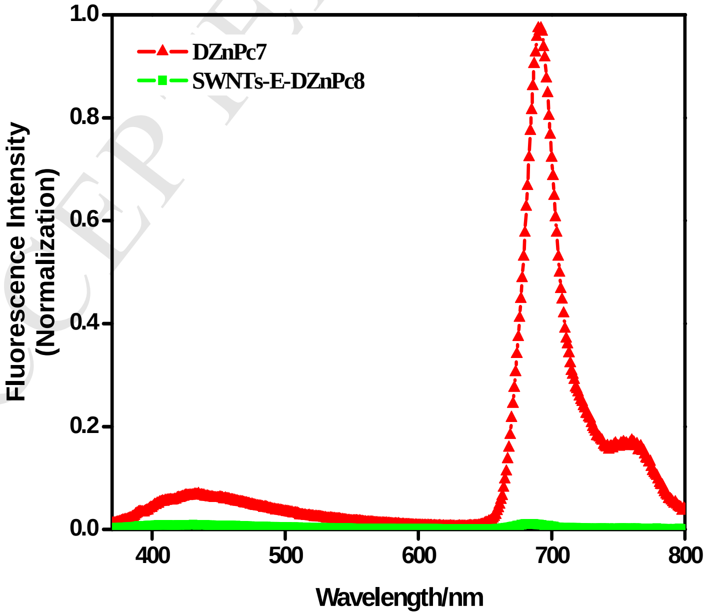

SI-Fig.10 Steady-state fluorescence spectra of DZnPc7, SWNTs-E-DZnPc8 in DMF at room temperature with matching absorption at the excitation wavelength (λ_{ex}= 350 nm, C= 2×10^{-5} moL/L).

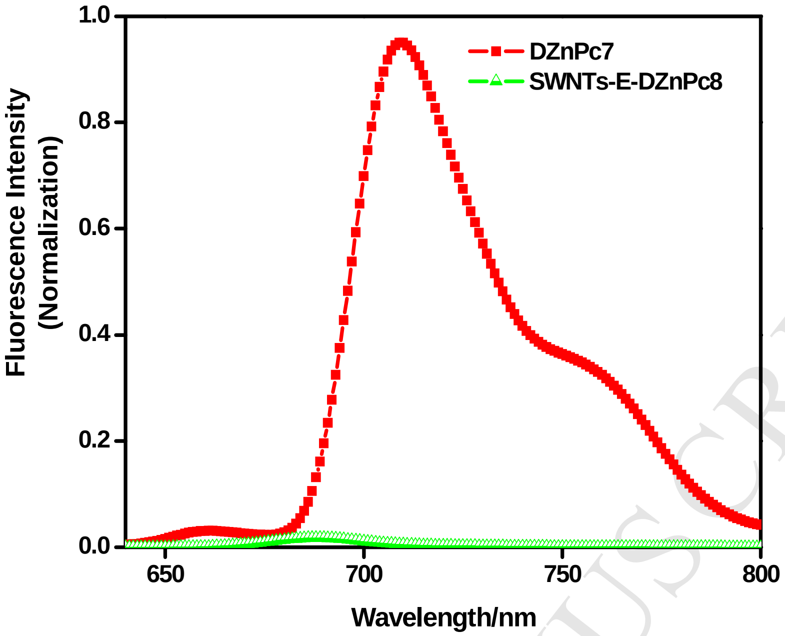

SI-Fig.11 Steady-state fluorescence spectra of DZnPc7, SWNTs-E-DZnPc8 in DMF at room temperature with matching absorption at the excitation wavelength (λ_{ex}= 610nm, C= 2×10^{-5} moL/L).

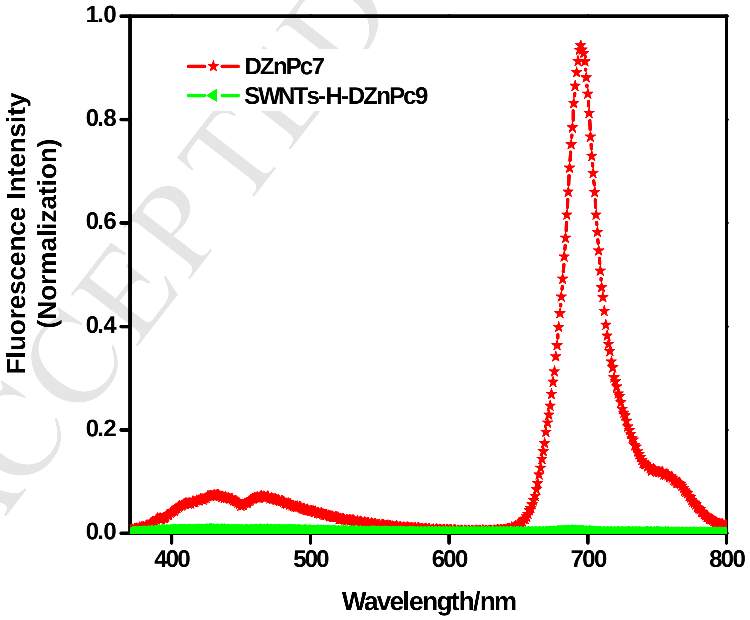

SI-Fig.12 Steady-state fluorescence spectra of DZnPc7, SWNTs-H-DZnPc9 in DMF at room temperature with matching absorption at the excitation wavelength (λ_{ex}= 350 nm, C= 2×10^{-5} moL/L).

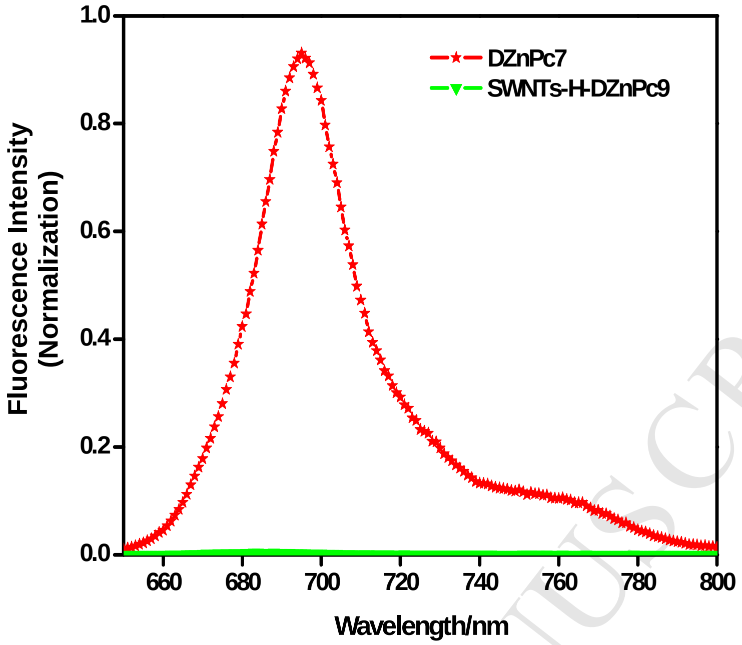

SI-Fig.13 Steady-state fluorescence spectra of DZnPc7, SWNTs-H-DZnPc9 in DMF at room temperature with matching absorption at the excitation wavelength (λ_{ex}= 610nm, C= 2×10^{-5} moL/L).

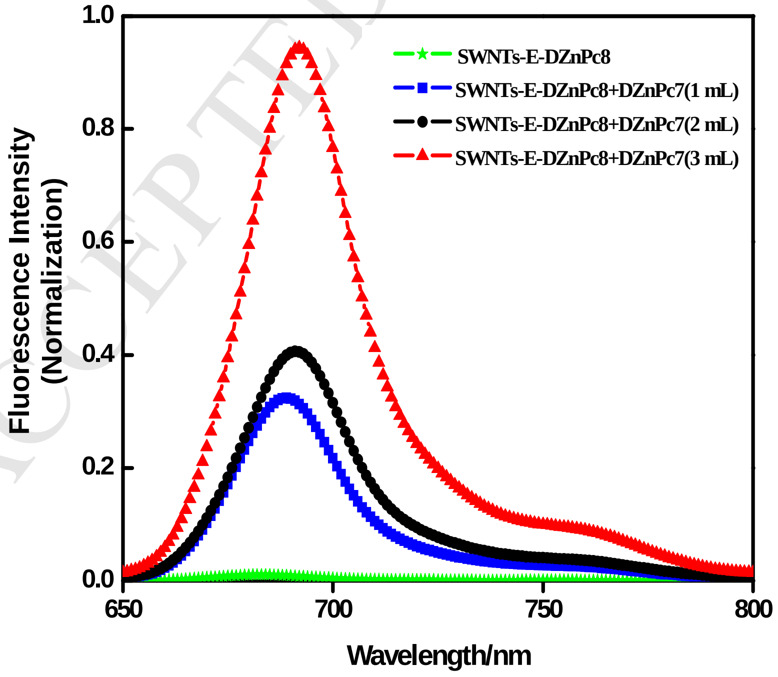

SI-Fig .14 The Steady-state fluorescence spectra of SWNTs-E-DZnPc8 after adding same concentration of free dendritic phthalocyanine DZnPc7 (0 mL, 1 mL, 2 mL, 3 mL) into the DMF solution

(λ_{ex}= 350 nm, $C_{DZnPc7\ and\ \ SWNTs\text{-}E\text{-}DZnPc8}$ = 2×10^{-5} moL/L).

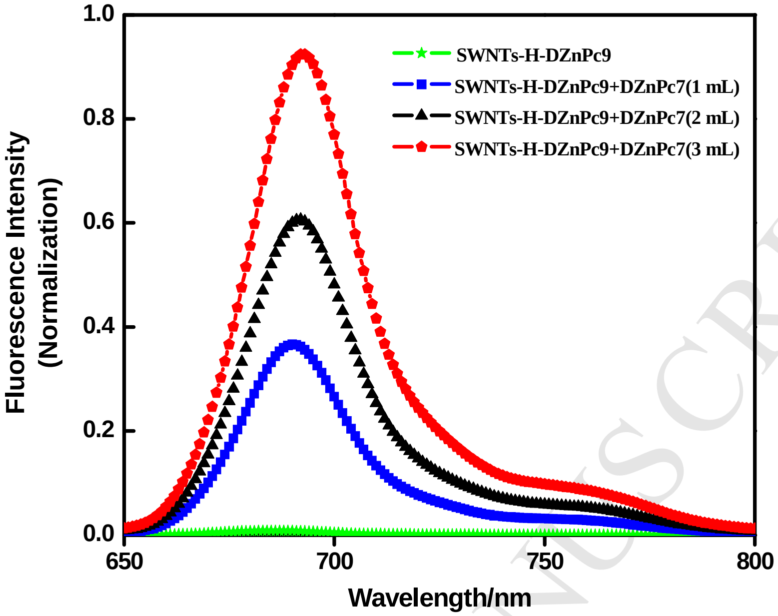

SI-Fig.15 The Steady-state fluorescence spectra of SWNTs-H-DZnPc9 after adding same concentration of free dendritic phthalocyanine DZnPc7 (0 mL, 1 mL, 2 mL, 3 mL) into the DMF solution (λ_{ex}= 610 nm, $C_{DZnPc7\ and\ \ SWNTs\text{-}E\text{-}DZnPc9}$ = 2×10^{-5} moL/L).

Highlights:

- Synthesis and characterization of a novel series of dendritic phthalocyanine-single-wall carbon nanotubes nanoconjugates using either ethylenediamine or hexamethylenediamine as the spacer linker.
- Intramolecular electron transfer could occur from phthalocyanines (donor) to single-wall carbon nanotubes (acceptor) during a photoinduced process.
- The electron transfer exchange rate and electron exchange efficacy between the dendritic phthalocyanines and single-wall carbon nanotubes increased with decreasing length of spacer linker.